



## Upregulation of autophagy in M2 macrophage by vitamin D alleviates crystalline silica-induced pulmonary inflammatory damage

Youjing Yang<sup>a</sup>, Shuhui Wei<sup>a</sup>, Kaimiao Chu<sup>a</sup>, Qianmin Li<sup>a</sup>, Yujia Zhou<sup>a</sup>, Yu Ma<sup>b</sup>, Lian Xue<sup>a</sup>, Hailin Tian<sup>a</sup>, Shasha Tao<sup>a,b,\*</sup>

<sup>a</sup> School of Public Health, Medical College of Soochow University, 199 Ren'ai Road, Suzhou 215123, China

<sup>b</sup> Chongqing University Central Hospital & Chongqing Emergency Medical Center, No. 1 Jiankang Road, Yuzhong District, Chongqing 400014, China

### ARTICLE INFO

Edited by Professor Bing Yan

#### Key words:

Vitamin D  
Silica  
Macrophage autophagy  
Pulmonary inflammatory injury

### ABSTRACT

Crystalline silica (CS) is a universal environmental pollutant, which causes a typical inflammatory lung injury. Vitamin D shows huge potential against particles-induced lung injury, while little known about the molecular mechanism involved in macrophage autophagy. In this study, we aim to identify the protective effects of vitamin D on CS caused lung inflammatory injury and clarify the detail mechanism. After exposure to CS (3 mg/mice in 50  $\mu$ l PBS), wildtype and Atg7<sup>fllox/fllox</sup> Lyz2-cre mice were treated with or without vitamin D<sub>3</sub> (40,000 IU/kg). The results indicated that exposure to CS caused an obvious lung injury, manifesting as pathological structural changes, macrophage-dominated inflammatory cell infiltration and increased pro-inflammatory cytokines. Remarkably, these damages were more serious in Atg7<sup>fllox/fllox</sup> Lyz2-cre mice. Vitamin D was found to inverse CS-induced inflammatory cell infiltration and restored anti-inflammatory M2 macrophages by inducing autophagy, which attenuated lung injury, as determined by decreased levels of apoptosis and inflammatory response. While, this effects of vitamin D were slashed in Atg7<sup>fllox/fllox</sup> Lyz2-cre mice. This study reveals the adverse effect of CS on lung tissue and the protective mechanism of vitamin D involved in M2 macrophages autophagy, which attenuates CS-caused lung injury.

### 1. Introduction

Crystalline silica (CS) is a considerable occupational hazard to those exposed workers. It is reported that there are approximately tens of millions of workers exposed to crystalline silica around the world (Lai et al., 2018; Leung et al., 2012). Except for traditional exposure routes such as mining, pottery and glass, an array of exposure circumstances continue emerging (Steenland and Ward, 2014; Barmania, 2016). Since inhalation of CS, it's impossible to remove it from lung tissue again (Du et al., 2019). Thus, the damage caused by CS is persistent. Many studies have identified that exposure to CS is closely related to pulmonary inflammation and fibrosis (Leung et al., 2012; Sayan and Mossman, 2016; The Lancet Respiratory, 2019). Inflammatory response is the beginning of crystalline silica-caused pulmonary fibrosis, which is induced by the recruitment and accumulation of multiple inflammatory cells (Dong and Ma, 2016; Li et al., 2017). Macrophage is the major regulator among these cells.

As the traditional innate immune cells, macrophages are reported to play a critical role in immunological homeostasis and defending lung inflammatory injury caused by various factors (Zhang et al., 2021; Li et al., 2021). Activated macrophages often express a mixed phenotype, and different micro-environmental stimuli can mediate macrophages to the indicated polarization (Mantovani et al., 2005; Shang et al., 2021). Currently, at least two distinct phenotypes of polarized macrophage are described: one called canonical activated (or pro-inflammatory) macrophages (M1) and the other called non-canonical activated (or anti-inflammatory) macrophages (M2). Disturbance in M1 vs. M2 balance is a hallmark of many inflammatory diseases (Hu et al., 2021).

During the invasion process of CS, macrophages suffering from inflammatory injury and apoptosis. Specifically, CS inhalation leads to the accumulation of reactive oxygen species (ROS), which induces inflammatory pathways and further causes mitochondrial dysfunction and apoptosis (Hamilton et al., 2008; Fazzi et al., 2014). Moreover, the apoptotic macrophages release massive ROS and inflammatory factors,

**Abbreviations:** BALF, Bronchial alveolar lavage fluid; CS, Crystalline silica; Cal, Calcitriol; CC3, Cleaved caspase-3; CQ, Chloroquine; GSH, glutathione; ROS, reactive oxygen species; PMA, phorbol-12-myristate-13-acetate; VD<sub>3</sub>, vitamin D<sub>3</sub>.

\* Corresponding author.

E-mail address: [sstao@suda.edu.cn](mailto:sstao@suda.edu.cn) (S. Tao).

<https://doi.org/10.1016/j.ecoenv.2021.112730>

Received 15 July 2021; Received in revised form 19 August 2021; Accepted 27 August 2021

Available online 31 August 2021

0147-6513/© 2021 The Author(s). Published by Elsevier Inc. This is an open access article under the CC BY license (<http://creativecommons.org/licenses/by/4.0/>).

causing excessive tissue injury (Zhang et al., 2014). Thus, modulation the accumulation of macrophages and protecting them from apoptosis become particularly significant.

Autophagy is a highly conserved process in biological evolution, maintaining intracellular homeostasis and cell self-renewal through degradation and recycling (Glick et al., 2010; Parzych and Klionsky, 2014). Increasing evidences have shown that autophagy also plays an important regulatory role in inflammation and immune process (Levine et al., 2011; Saitoh and Akira, 2016; Deretic et al., 2013; Qi et al., 2019). Moreover, there are intrinsic links between autophagy and macrophage function revealed by accumulated evidences. On the one hand, macrophages are one of the major bridges linking autophagy and immunity (Clarke and Simon, 2019; Shibutani et al., 2015). On the other hand, autophagy is involved in the regulation of macrophage polarization and down-regulation of inflammation (Ilyas et al., 2016; Liu et al., 2015). Peng Qiu et al. found that decreased macrophage autophagy caused by obesity leads to liver inflammation and injury, which indicates that the deficiency of macrophage autophagy may be the basis of inflammatory disease (Qiu et al., 2019).

Our previous studies as well as others' showed that vitamin D, an endocrine hormone, has immunomodulatory potential in various inflammatory diseases (Guo et al., 2021; H. Zhang et al., 2019). Moreover, it was demonstrated that vitamin D conferred survival and fitness to cells through modulation of autophagy (Berridge, 2017; Holmes, 2017; Høyer-Hansen et al., 2010). It could protect against particles-caused lung injury through induction of autophagy in an Nrf2-dependent manner (Tao et al., 2019). Also, Das, Lopa M et al. suggested that vitamin D alleviated UV-induced skin inflammatory injury by increasing autophagy in M2 macrophages (Das et al., 2019). However, the role of vitamin D in regulating M2 autophagy in CS-induced lung inflammatory injury still less known. In this study, we disclosed that the anti-inflammation effects of vitamin D are correlated with its function on macrophage autophagy. Our results suggest that exposure of CS causes macrophage polarizing to M1, secreting pro-inflammatory cytokines and leading to tissue damage. While the damage caused by CS could be attenuated by vitamin D, manifesting as the reversed ratio of M1/M2 and up-regulated M2 autophagy. The results may provide an effective protection to CS-caused lung inflammatory injury.

## 2. Material and Methods

### 2.1. Animals and treatments

6–8-week-old C57BL/6 mice were purchased from SLAC Laboratory Animal Co. Ltd. Atg7<sup>lox/lox</sup> mice were gifts from Dr. Jianrong Wang, Soochow University School of Medicine (Cao et al., 2015; Komatsu et al., 2005). To generate myeloid-specific Atg7 deficient mice (design as Atg7<sup>-/-</sup>), Atg7<sup>lox/lox</sup> mice were crossed with Lyz2-Cre mice (Cyagen, Guangzhou, China) and both male and female mice were used for experiments. All mice received standard laboratory diet and maintained in 12 h light/dark cycle, climate-controlled and pathogen-free rooms. Mice handling in this study followed the Guide for the Care and Use of Laboratory Animals and the study protocols were approved by Soochow University Institutional Animal Care and Use Committee. After adaptively fed for 1 week, both wildtype and Atg7<sup>-/-</sup> mice were randomly separated into four groups (n = 6 per group): control (Ctrl), crystalline silica (CS), vitamin D (VD<sub>3</sub>), combination (VD<sub>3</sub> + CS).

### 2.2. Crystalline Silica preparation and drug dosage regimen

Crystalline Silica particles (Quartz DQ 12) were purchased from Doerentrup Quarz GmbH (Germany). The content of the free SiO<sub>2</sub> dust was more than 99%. Distribution of particle size is as follows: 90% less than 2.3 μm, 50% less than 1.1 μm, and 10% less than 0.6 μm. Crystalline silica preparation was according to our previous studies and others (Li et al., 2017; Tao et al., 2019). Specifically, CS particles were weighed

and ground, boiled in 1 N hydrochloric acid, washed, dried, and suspended in sterile saline to prepare a CS suspension with the concentration of 3 mg/50 μl. Suspensions were sonicated for 10 min and fully blended with a vortex before use.

For the exposure of CS, mice were anesthetized and instilled with fully blended CS suspension intratracheally. Vitamin D<sub>3</sub> (VD<sub>3</sub>) was dissolved in corn oil with the final concentration of 40,000 IU/kg and administrated by a single intraperitoneal (i.p.) injection after instillation of silica suspension according to our previous studies (Tao et al., 2019). Mice were weighed and sacrificed one week after CS instillation.

### 2.3. Bronchoalveolar lavage fluid (BALF), primary macrophages isolation and tissue collection

Mice were euthanized and BAL fluid (BALF) was obtained by lavaging the lung with 1 ml PBS (Invitrogen) through tracheal cannula, then cells and supernatant were separated as described previously (Moreno-Vinasco et al., 2014). Briefly, total cell amount was determined by TC20 automated cell counter (BioRad, California, USA) followed by collecting from centrifuged BALF. A small portion of cells were used to identified macrophages with standard morphologic criteria by Wright-Giemsa staining. The remaining cells were used by 2 h-culture in the DMEM with 10% FBS 37 °C to obtain pure primary macrophages for further experiments. Supernatants and tissues were harvested for next step analyses.

### 2.4. RNA extraction and real-time RT-PCR

RNA was collected using TRIzol from CWBIO (Beijing, China). Equal amounts of RNA were used to generate cDNA using a HiFiScript cDNA synthesis kit following the manufacturer's instructions (CWBIO). ABI 7500 (Applied Biosystems) was used to evaluate RNA expression using an UltraSYBR Mixture qPCR kit (CWBIO). Primer sequences are listed as follows: m-TNFα: forward (agccccagctgtatcctt), reverse (ggtcactgtcccagcatctt); m-TGFβ: forward (gactctccactgcaagacc), reverse (gactggcagccttagtttg); m-IL6: forward (ccggagaggagacttcacag), reverse (tccacgatttcccagagaa); m-IL10: forward (aaggaccagctggacaacat), reverse (tcatttccgataaggcttg) and m-β-actin: forward (aagccaaccgtgaaagat), reverse (gtggtacgaccagggcacaac).

The real-time PCR conditions were: initial denaturation (95 °C, 10 min), 40 cycles of amplification (95 °C, 10 s; 60 °C, 30 s; 72 °C, 30 s), melting curve (95 °C, 15 s; 60 °C, 1 min; 95 °C, 15 s), cooling cycle (60 °C, 15 s) with 96-well PCR plates (Nest, 402101). Mean crossing point (Cp) values and standard deviations (SD) were determined. Cp values were normalized to the respective Cp values of the mouse β-actin. Data are presented as a fold change in gene expression compared to control group.

### 2.5. Hematoxylin & Eosin (H&E) and Immunohistochemical (IHC) staining

Tissue sections were baked and deparaffinized for H&E and IHC staining. H&E staining was performed for pathological analysis. Immunohistochemical (IHC) analysis was performed as previously described (Tao et al., 2013). Briefly, staining was performed using EnVision+System-HRP kit (Dako, Denmark) according to the manufacturer's instructions. First, antigen retrieval was performed by boiling the slides with retrieval solution (citric acid monohydrate 2.1 g/l in H<sub>2</sub>O, pH = 6.0) three times for 5 min each time and tissue sections were then exposed to 3.5 M HCl for 15 min at room temperature. Next, tissue sections were washed with PBS three times for 5 min each time and treated with 0.3% peroxidase to quench endogenous peroxidase activity. Finally, tissue sections were blocked for 30 min with 5% normal goat serum for followed by 2 h incubation with various primary antibodies at 1:100 dilutions at room temperature.

## 2.6. Detection of 25(OH)D<sub>3</sub> and Calcium detection

Vitamin D ELISA Kit (E-EL-0012c) and Calcium Colorimetric Assay Kit (E-BC-K103-M) were purchased from Elabscience. Tissues were washed with pre-cooling PBS to remove residual blood. Then the sheared tissues were added corresponding volume of PBS and ground with sonication. Next, the homogenate was centrifuged at 5000 g for 10 min at 4 °C to obtain supernatant for detection. The concentration of 25(OH)D<sub>3</sub> in serum and lung tissue, as well as serum calcium levels were detected according to the manufacturer's instructions.

## 2.7. Chemicals, antibodies, and cell culture

Vitamin D<sub>3</sub> (VD<sub>3</sub>; 731285), Calcitriol (active form of vitamin D; Cal; D1530), and Chloroquine (CQ), Rapamycin were purchased from Sigma-Aldrich (Dallas, Texas, USA). Primary antibodies against LC3 (sc-398822), P62 (sc-28359), ATG7 (sc-376212), Nrf2 (sc-13032), GCS (sc-55586), NQO1 (sc-32793), GAPDH (sc-32233), Cleaved caspase-3 (sc-56053), NOS-2 (sc-7271) and Arg-1 (sc-166920) were purchased from Santa Cruz (Texas, USA). Horseradish peroxidase (HRP)-conjugated secondary antibodies were from Immunoway (anti-mouse: RS0001, anti-rabbit: RS0002, Plano, Texas, USA). Alexa Fluor 488, 594 anti-rabbit, and anti-mouse IgGs were from Santa Cruz. Flow cytometric antibodies against APC Anti-mouse F4/80 (20–4801) was obtained from TONBO biosciences (San Diego, CA, USA); PE anti-mouse CD86 (105008), PE/Cy7 anti-mouse CD206 (141720), TruStain FcX™ anti-mouse CD16/32 (101320) antibodies were from Biolegend (San Diego, CA, USA). Human THP-1 acute monocytic leukemia cells was from ATCC. Cells were cultured in RPMI 1640 containing 10% FBS (Hyclone), 0.1% gentamycin (Invitrogen) and differentiated by 5 ng/ml phorbol-12-myristate-13-acetate (PMA, Sigma) in a humidified incubator (37 °C; 5% CO<sub>2</sub>).

## 2.8. Immunoblot analysis

Cells and tissues were lysed in Laemmli buffer (62.5 mM Tris-HCl [pH 6.9]) 3% SDS, 10% glycerol, 5% Beta-mercaptoethanol, and 0.1% bromophenol blue. Cell lysates were sonicated after boiled 10 min. Denatured lysates were electrophoresed through SDS-polyacrylamide gel and subjected to immunoblot analysis. The relative immunoblot bands are compared using the prestained protein marker (Vazyme Biotech Co., Ltd, MP102-01) and the intensities were quantified by the Syngene gel documentation system and GeneTools software from Syngene (Frederick, MD, USA).

## 2.9. Indirect immunofluorescence staining

Cells on round glass coverslips (Fisher Scientific) were fixed with pre-chilled methanol. After blocked with 5% BSA/PBS, slides were incubated with primary antibody (1 h) and secondary antibody (50 min), and mounted with anti-fade mounting solution (Invitrogen). Images were captured with a fluorescence microscope (LEICA DM 2500).

## 2.10. Flow cytometry assay

Cells were collected from BALF and 40ul 1% FBS/PBS was added. After blocked with CD16/32, APC-F4/80, PE/Cy7-CD206 or PE-CD86 were added and incubated 1 h at 4 °C in the dark. The fluorescence signals were measured by flow cytometry (BD FACSCantoII) and data were analyzed by FlowJo software.

## 2.11. Apoptosis

Harvested cells were resuspended with 100ul Binding buffer, then 5ul Annexin V-FITC and 10ul PI were added. After gently mixed, cells were incubated for 15 min in the dark. Then 400ul Binding buffer was

added, the fluorescence intensity was detected by flow cytometry within 1 h.

## 2.12. Glutathione assays

The levels of GSH and GSSG were detected using a GSH and GSSG Assay kit (Beyotime, China). The cells were treated according to the manufacturer's instructions and measurements were recorded using a microplate reader (Synergy HT, BioTek Instruments Inc.) at 412 nm. The experiment was conducted in duplicates in three independent repeats.

## 2.13. Gene set enrichment analysis (GSEA)

We created a rank of the genes using a fold change which was calculated by limma package in R software (version 4.0.4) (Ritchie et al., 2015). The pre-ranked GSEA was performed utilizing clusterProfiler package, with "c5.go.bp.v7.4.entrez.gmt" and "c7.immunesigdb.v7.4.entrez.gmt" downloaded from the Molecular Signature Database (MSigDB, <http://software.broadinstitute.org/gsea/msigdb/index.jsp>) regarded as the reference gene sets (Yu et al., 2012). The GSEA results ( $p$  value < 0.05) were plotted using enrichplot package (H. Zhang et al., 2019; C. Zhang et al., 2019).

## 2.14. Statistics

All related data are presented as the mean±SEM of three independent experiments performed in triplicate. Comparisons between two groups were calculated by two-tailed Student's *t*-test, and significant differences between multiple groups were evaluated by one-way analysis of variance with Tukey's honestly significant difference (HSD) *post hoc* testing using GraphPad Prism 8 software (La Jolla, California, USA). The test statistics have been transformed into adjusted  $p$  values following Turkey multiple comparison testing. A value of  $p < 0.05$  was considered to be significant.

## 3. Results

### 3.1. Macrophages accumulation is involved in CS-induced pulmonary inflammatory injury

Macrophages are well known as effective scavengers. To investigate the status of macrophages during the invasion of CS, we conducted an *in vivo* model. First, by observing the morphology of lung tissue, we found that compared to the control group, CS exposure caused obvious lung injury, manifesting as infiltration of inflammatory cells and thickened alveolar septal in lung tissue (Fig. 1A). Next, cells from BALF were measured and calculated with microscope and flow cytometry. The results showed that CS exposure led to macrophages accumulation (Fig. 1B-C). Moreover, macrophages from CS exposed mice demonstrated a shift towards M1 phenotype, significantly suppressing the ratio of M2 to M1 macrophages in the BALF as shown in Fig. 1D. M1 macrophages are characterized by a pro-inflammatory phenotype, which secretes pro-inflammatory cytokines and then causes oxidative stress and tissue inflammatory injury. Thus, we next detected relative levels of inflammatory cytokines and other indicators. qRT-PCR analysis showed the increased mRNA levels of pro-inflammatory cytokines such as IL-6 and TNF- $\alpha$  after CS exposure (Fig. 1E). At the same time, CS exposure increased total protein levels in BALF supernatant (Fig. 1F). Besides, the up-regulated expression of cleaved caspase-3 (CC3) in lung tissue also confirmed CS-caused serious lung injury (Fig. 1G). Taken together, these results indicated that CS exposure triggers M1 macrophages accumulation and causes pronounced inflammatory injury.

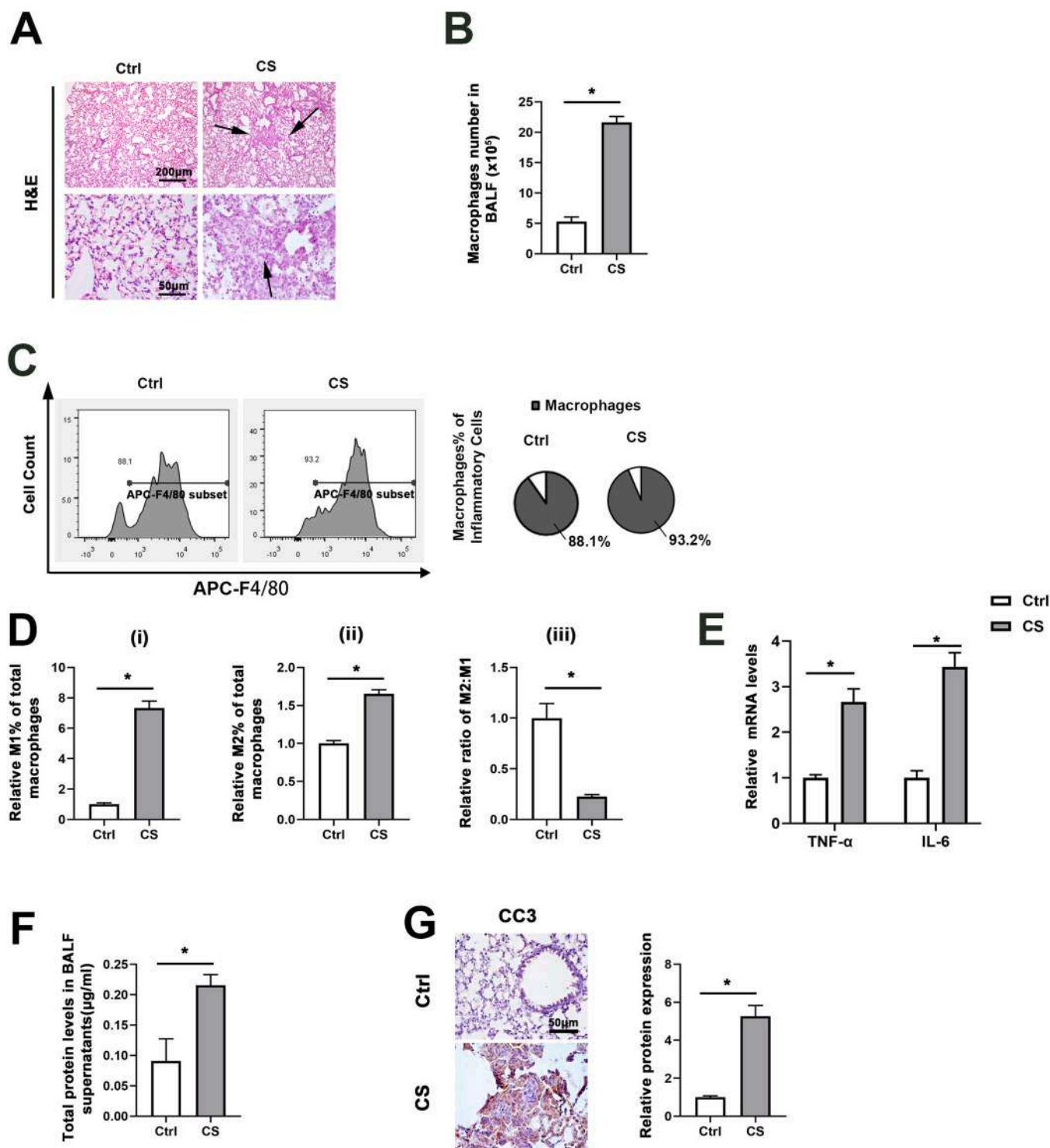


**Fig. 1.** Crystalline silica induced lung injury via accumulation of macrophages. (A) H&E staining of lung tissue (n = 6, Black arrows indicate inflammatory cell nodules). (B) The proportion of macrophages among the total cells in BALF from each treatment group. (C) Flow cytometry analysis on the ratio of macrophage in the total cells of BALF detected with APC labels F4/80 antibody. (D) The expression of CD86 (M1 biomarker) and CD206 (M2 biomarker) were detected by flow cytometry with PE-CD86 and PE-Cy7-CD206 antibodies from the above APC-F4/80 detected macrophages. Graphical representation of (i) M1 of total macrophages, (ii) M2 of total macrophages and (iii) ratio of M2 to M1 macrophages. Results are expressed as mean $\pm$ SEM (\**p* < 0.05, Ctrl vs. CS). (E) mRNA of macrophages purified from mice BALF with the indicated treatments was extracted. The expression of TNF- $\alpha$  and IL-6 were measured by qRT-PCR analysis. Results were expressed as mean $\pm$ SEM (n = 6; \**p* < 0.05, Ctrl vs. CS). (F) Total protein levels in BALF (n = 6). (G) IHC staining of CC3 of lung tissue from the indicated treatments was performed, representative images and quantification were shown. Results were expressed as mean $\pm$ SEM (n = 6; \**p* < 0.05, Ctrl vs. CS).

3.2. Vitamin D inverses CS-induced macrophages infiltration and restores anti-inflammatory M2 macrophages

In order to explore the anti-inflammation effect of vitamin D, we first conducted relative bioinformatic analysis. RNA-seq data of apparently normal human lung tissues were obtained from GTEx projects datasets (<https://www.gtexportal.org/>). Among them, which expressing VDR and CYP24A1 above the tissue median were classified as "high level of vitamin D signaling". Similarly, another were classified as "low level of vitamin D signaling" (Fig. 2A). GSEA of GOBP between the "high level" and "low level" group reveals that signatures representative of inflammation are significant in the "low level" group, suggesting the level of vitamin D signaling may be correlated with pulmonary inflammation

(Fig. 2B). Next, we measured the levels of vitamin D and calcium both in serum and lung tissue. The results showed that the levels of vitamin D were significantly increased both in serum and lung tissue after administration of vitamin D and the serum  $Ca^{2+}$  had a mild increase as well (Figs. 2C-D, S1A), and no hypercalcemia were observed. Followed by the above results that CS exposure caused lung inflammation by increasing the macrophages infiltration, especially M1, we sought to determine whether vitamin D intervention could alter the macrophage infiltration in this CS exposure model. As expected, CS-induced macrophages infiltration was reversed (Fig. 2E). Additionally, flow-cytometric analysis indicated that compared to CS exposure group, intervention with vitamin D restored the relative abundance of M2 macrophages and reduced M1 macrophages in the BALF (Fig. 2F). In accordance with the

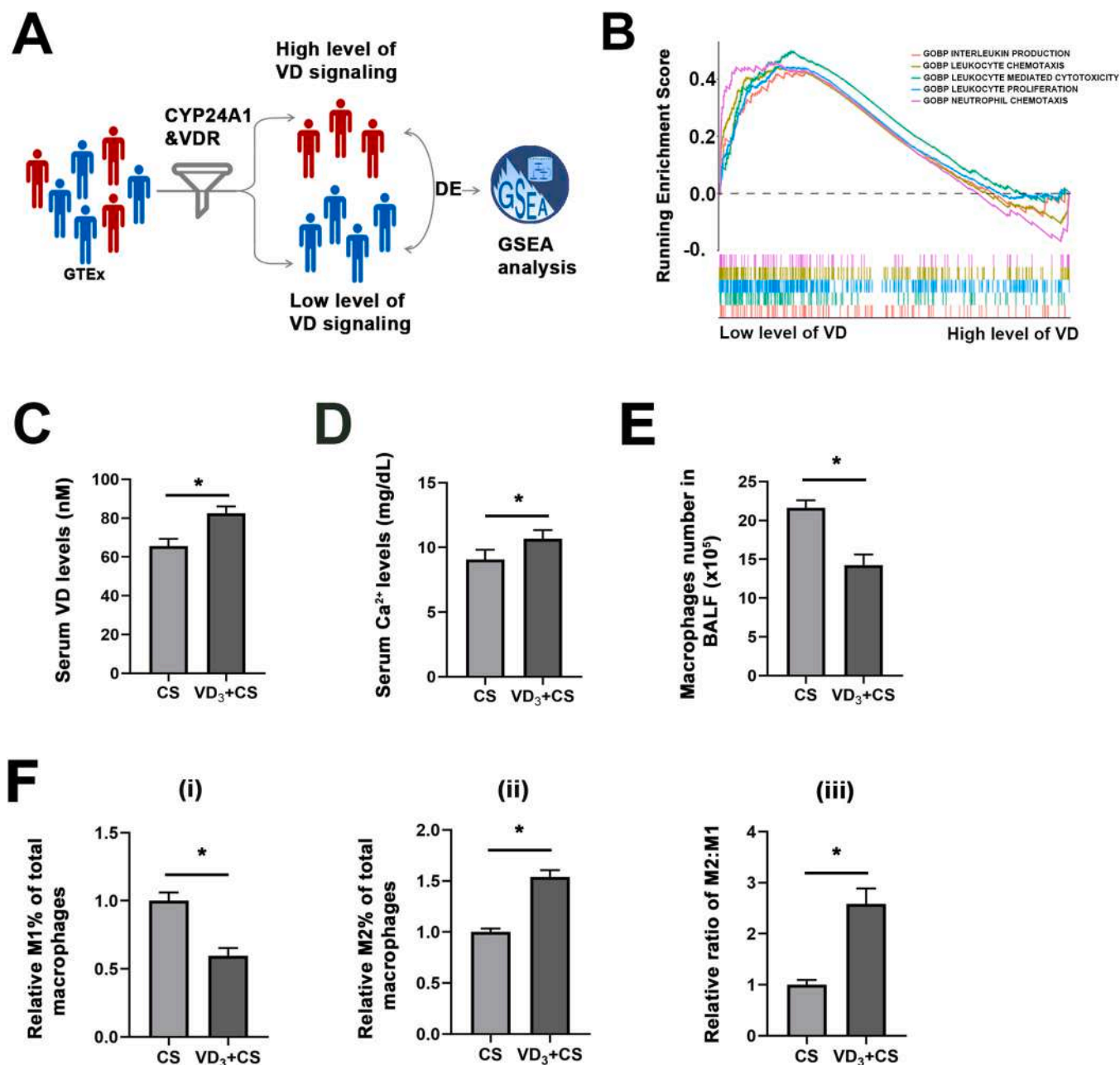
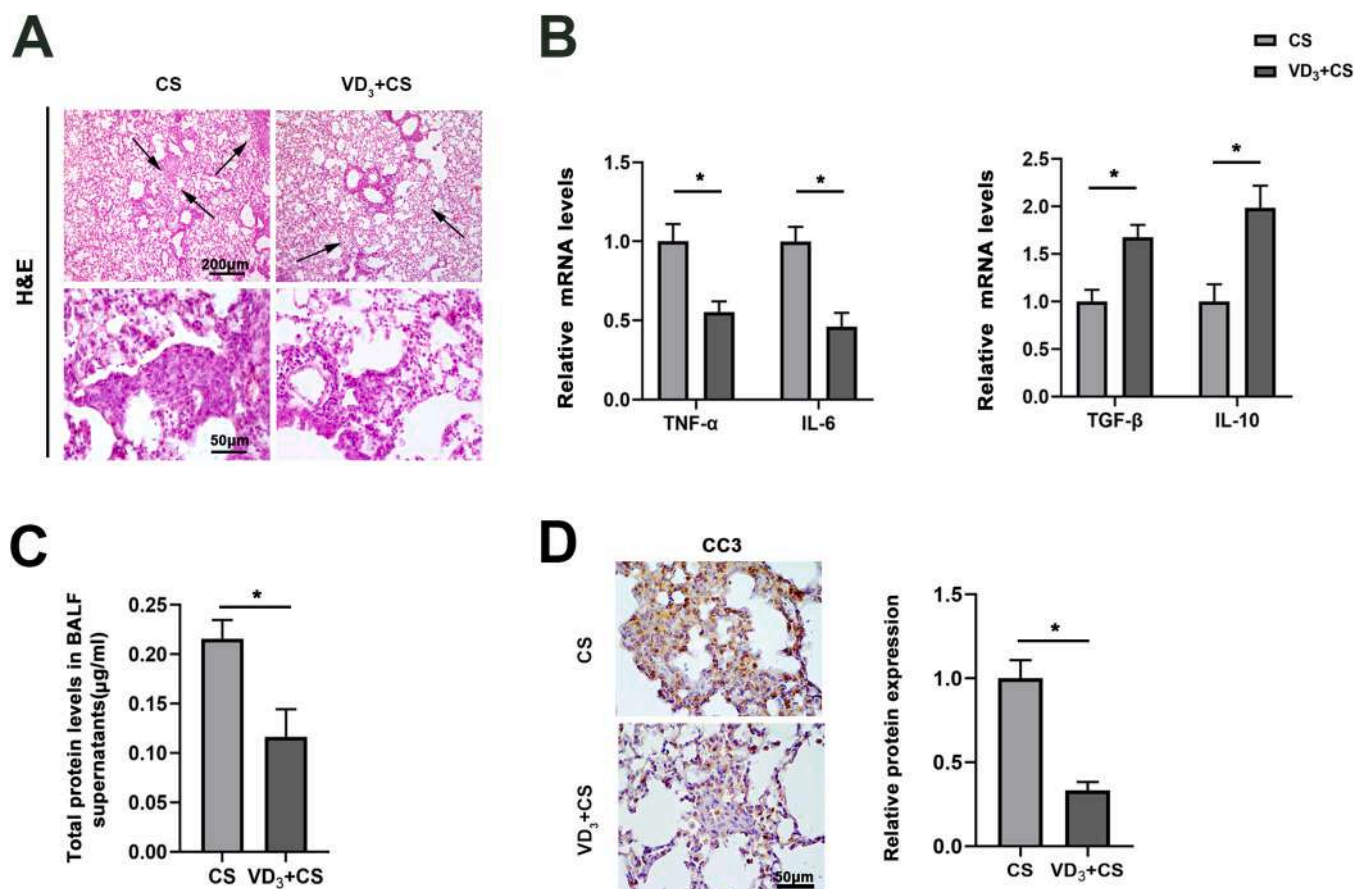


Fig. 2. Vitamin D alters the ratio of M1 to M2. (A) Segregating lung samples from the GTEx dataset of healthy post-mortem donors into lung tissues with high level and low level of vitamin D signaling. (B) GSEA analysis of 'low vs. high level of vitamin D signaling groups', showing 5 significant biological processes correlated with inflammatory response. (C) Serum vitamin D<sub>3</sub> and (D) Calcium concentration of indicated treatment groups (n = 6). (E) Number of macrophages in the mice BALF from each treatment group (n = 6). (F) (i) M1 of total macrophages, (ii) M2 of total macrophages (iii) ratio of M2 to M1 macrophages. Results were expressed as mean±SEM (n = 6; \*p < 0.05, CS vs. VD<sub>3</sub> + CS).



**Fig. 3. Vitamin D alleviates crystalline silica-induced lung injury.** (A) H&E staining of lung tissue ( $n = 6$ , Black arrows indicate inflammatory cell nodules). (B) mRNA of macrophages purified from mice BALF with the indicated treatments was extracted. The expression of TNF- $\alpha$ , IL-6, TGF- $\beta$  and IL-10 were measured by qRT-PCR analysis. Results were expressed as mean  $\pm$  SEM ( $n = 6$ ; \* $p < 0.05$ , CS vs. VD<sub>3</sub> + CS). (C) Total protein levels in BALF ( $n = 6$ ). (D) IHC staining of CC3 of lung tissue from the indicated treatments was performed, representative images and quantification were shown. Results were expressed as mean  $\pm$  SEM ( $n = 6$ ; \* $p < 0.05$ , CS vs. VD<sub>3</sub> + CS).

result of flow-cytometric analysis, IF staining also suggested that vitamin D promoting macrophages polarizing to M2 (Fig. 4C). The combined data suggested that the shift towards an increased inflammatory M1 population caused by CS was altered with vitamin D treatment.

### 3.3. Vitamin D alleviates CS-induced pulmonary inflammatory followed by the restored anti-inflammatory M2 macrophages

Based on the results that vitamin D increased the population of anti-inflammatory M2 macrophages, we next evaluated its effect on CS-caused injury. HE staining showed that vitamin D attenuated CS-induced lung tissue injury, manifesting as alleviating the lung tissue damages (Fig. 3A). Besides, the protein levels of BALF supernatant from vitamin D intervention mice were lower than that of CS group (Fig. 3C). At the same time, relative CC3 expression also decreased after vitamin D administration (Fig. 3D). Moreover, we detected relative cytokines using qRT-PCR. The data suggested that the mRNA levels of pro-inflammatory cytokines such as IL-6, TNF- $\alpha$  were down-regulated, while the anti-inflammatory cytokines such as IL-10, TGF- $\beta$  were up-regulated after vitamin D treatment (Fig. 3B). The implication of these results was that vitamin D shows protective effects on CS-induced pulmonary injury.

### 3.4. Vitamin D induces autophagy in M2 macrophages and ameliorates CS-induced macrophages apoptosis

Next, we sought to explore the detail mechanism of vitamin D on the

regulation of macrophages. Differentiated THP-1 cells were treated with Cal 24 h with or without chloroquine (CQ, classical autophagy inhibitor) intervention. p62, an autophagy substrate was up-regulated with CQ treatment. However, it was modestly decreased after Cal administration and the expression of co-treatment group was increased compared to Cal alone, which suggested that Cal induced autophagy. Consistently, relative levels of LC3 also indicated that Cal could up-regulate autophagy *in vitro* (Fig. 4A). To confirm these results, cells were transfected with a tandem mouse red fluorescent protein (mRFP)-GFP-LC3 construct and either left untreated or treated with 50  $\mu$ M CQ, 100 nM Rapamycin and Cal 50 nM. GFP fluorescence is quenched in acidic environments like lysosome or autolysosome, whereas mRFP is more stable. Therefore, colocalization of both GFP and RFP fluorescence (yellow puncta in merged image) indicates an autophagosome that has not yet fused with a lysosome or where acidification of the lysosome is disrupted such as CQ treatment. In contrast, RFP alone with no GFP corresponds to an autolysosome like rapamycin treatment. Interestingly, red puncta were observed in cells treated with 50 nM Cal. These results support the regulation of Cal on autophagy process is similar to rapamycin to increase formation of autophagosomes (Fig. 4B). Additionally, mice BALF purified macrophages were stained to detect and co-localize LC3 with M2 marker Arg-1. After vitamin D treatment, the ratio of Arg-1<sup>+</sup>LC3<sup>+</sup> cells are higher than the ratio of NOS-2<sup>+</sup>LC3<sup>+</sup> cells (yellow puncta in the merged image), which indicates that vitamin D activated autophagy mainly in M2 macrophages (Fig. 4C). Finally, relative levels of cell apoptosis showed that vitamin D protects macrophages from CS-induced injury. These data revealed that vitamin D could up-regulate the

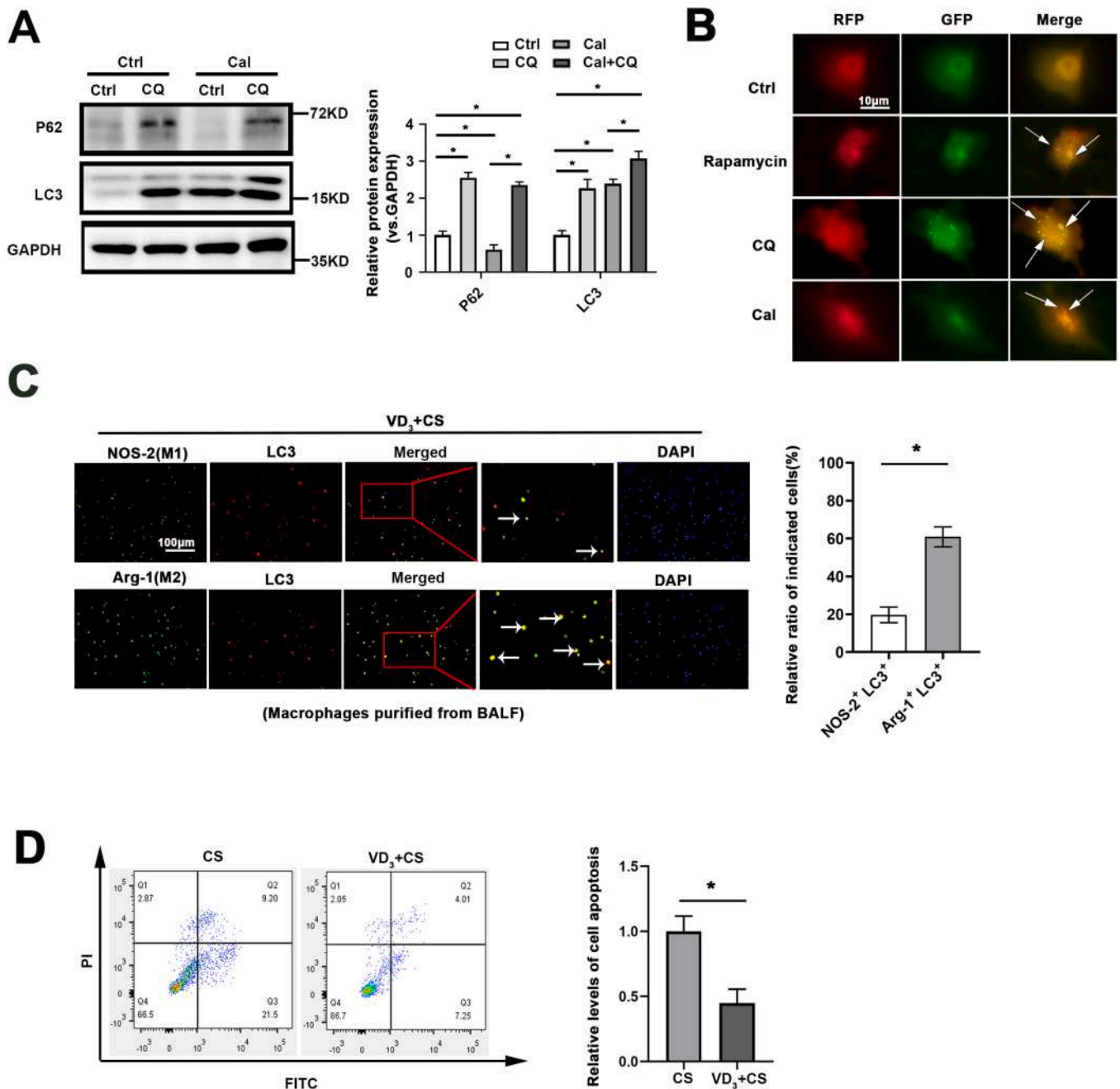


**Fig. 4. Vitamin D enhances M2 autophagy and relieves crystalline silica-induced cell apoptosis.** (A) THP-1 cells were either left untreated or treated with Cal (50 nM), CQ (50  $\mu$ M) for 24 h. Cell lysates were subjected to immunoblot analysis and the blots were quantified (\* $p$  < 0.05, Ctrl vs. Treatments, Cal vs. Cal+CQ). (B) Followed by transfected with a tandem mRFP-GFP-LC3 construct for 24 h, THP-1 cells were left untreated or treated with 100 nM rapamycin, 50  $\mu$ M CQ, or 50 nM Cal for another 24 h. Live-cell images were captured. (C) The representative immunofluorescence image of Arg-1(M2)<sup>+</sup> LC3<sup>+</sup>, NOS-2(M1)<sup>+</sup> LC3<sup>+</sup> of macrophages of fluorescence intensity and relative cell ratio were shown. (D) Macrophages purified from the indicated treatment groups were harvested to detect the levels of Annexin-FITC and PI by flow cytometry assay. The representative images and quantification of cell apoptosis were shown (\* $p$  < 0.05, CS vs. VD<sub>3</sub> +CS). (For interpretation of the references to colour in this figure, the reader is referred to the web version of this article.)

autophagy in M2 macrophages, which ameliorates CS-induced macrophages apoptosis.

### 3.5. Deficiency of autophagy macrophage erodes vitamin D's capacity to attenuate inflammation

Base on those above results, we hypothesized that the protective effect of vitamin D maybe base on the induction of macrophage autophagy. To further confirm the role of macrophage autophagy in the prevention of vitamin D against CS-mediated pulmonary injury, we

recapitulated the CS model in myeloid-specific Atg7 deficient (Lyz2-Cre-Atg7<sup>fl/fl</sup>, design as Atg7<sup>-/-</sup>) mice. The histopathology showed a pronounced phenotype with more infiltrated inflammatory cells and thicker alveolar septal in Atg7<sup>-/-</sup> mice compared to Atg7<sup>+/+</sup> mice following CS exposure. Moreover, vitamin D did not rescue Atg7<sup>-/-</sup> mice from CS induced damage and inflammation compared to the wildtype mice (Fig. 5A). We also observed comparable phenomenon in the protein level of BALF supernatant that vitamin D attenuated CS-induced up-regulation of total protein levels in wildtype mice while showed no effect in Atg7<sup>-/-</sup> mice (Fig. 5B). Consistently, relative mRNA levels of pro-

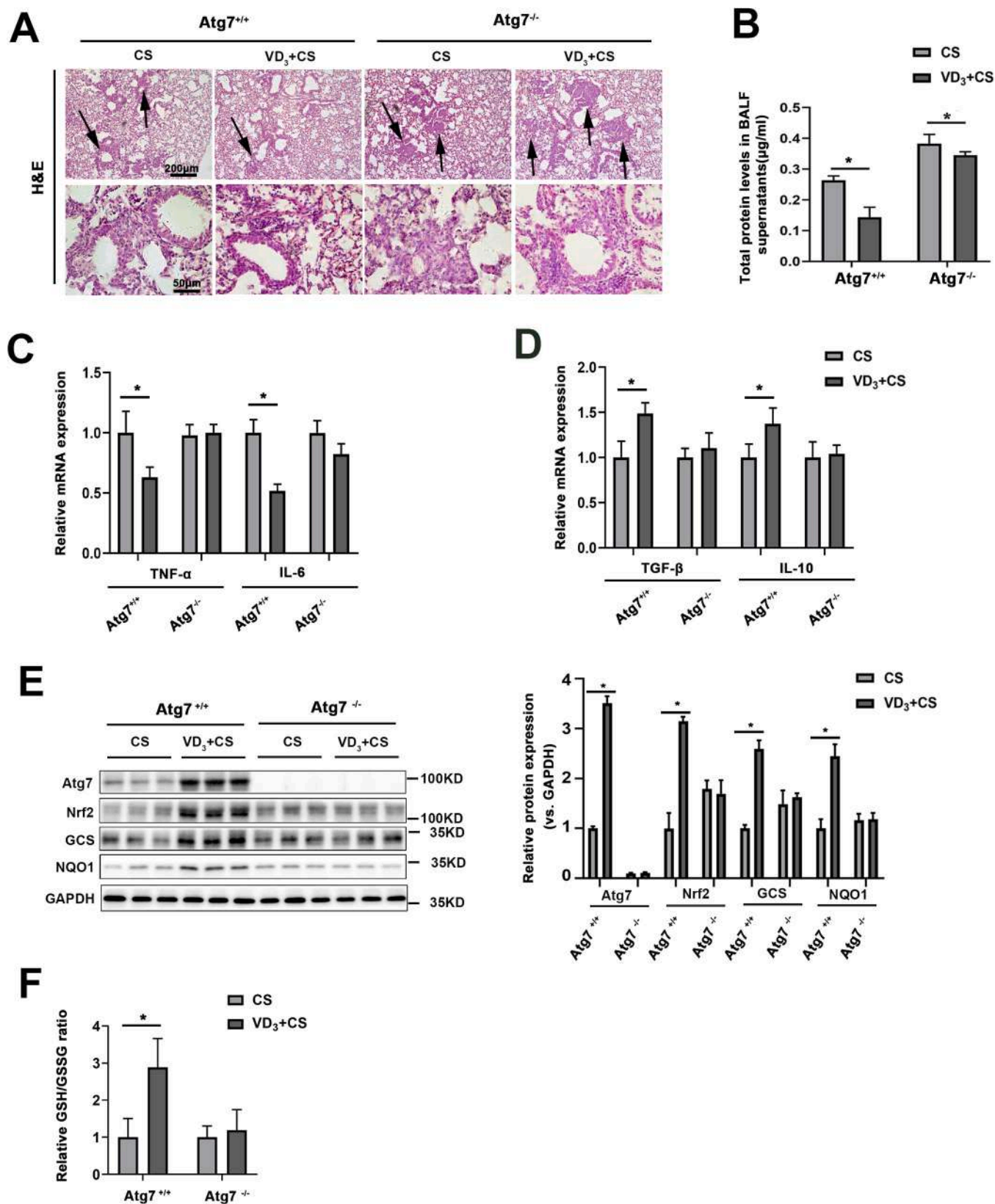


**Fig. 5.** Inhibition of autophagy by depleting Atg7 in macrophages abolishes vitamin D's protection of crystalline silica-induced lung inflammatory injury. (A) H&E staining of lung tissue from Atg7<sup>+/+</sup> and Atg7<sup>-/-</sup> mice with the indicated treatments were performed (n = 6, Black arrows indicate inflammatory cell nodules). (B) Total protein amount in BALF supernatant were measured. (C, D) The mRNA of BALF purified macrophages above were extracted, and relative expression of TNF-α, IL-6, TGF-β and IL-10 were measured with qRT-PCR analyses. Results are expressed as mean±SEM (n = 6; \*p < 0.05, CS vs. VD<sub>3</sub> +CS). (E) Macrophages purified from Atg7<sup>+/+</sup> and Atg7<sup>-/-</sup> mice BALF were harvested for immunoblot analysis, and the intensity of the indicated bands were quantified (\*p < 0.05, CS vs. VD<sub>3</sub> +CS). (F) Purified macrophages from indicated group were harvested for the measurement of GSH/GSSG ratio. Results were expressed as mean±SEM (\*p < 0.05, CS vs. VD<sub>3</sub> +CS).

inflammatory and anti-inflammatory cytokines also indicated that Atg7 ablation mice exhibited more serious inflammatory injury and the protective effect of vitamin D was impaired (Fig. 5C-D). Besides, the anti-inflammatory capacity was measured. Nrf2, the classical transcription factor that regulates the antioxidant defense response against the harmful effects of ROS was examined through western blot. Also, vitamin D up-regulated the Nrf2 signaling pathway, while depletion of Atg7 diminished the effect of vitamin D on regulating Nrf2 signaling pathway (Figs. 5E, S1B). Consistently, relative ratio of GSH/GSSG also showed that inhibition of autophagy impaired vitamin D's capacity of antioxidant (Fig. 5F). Overall, these findings supported that vitamin D protected against CS-induced lung injury in an autophagy dependent manner.

#### 4. Discussion

Vitamin D is well known for the modulation of mineral homeostasis, while its nonclassical actions especially the anti-inflammation activity has drawn more and more attention. Regrettably, few studies focus on the effect of vitamin D on CS-induced lung inflammatory injury. In this study, the protective role and detailed mechanism of vitamin D in CS exposure-induced lung injury were investigated. First, animal study revealed that CS exposure caused a series of inflammatory responses, including inflammatory cell infiltration, alveolar septal thickening and cell apoptosis due to the accumulation of macrophages, especially M1 macrophages (Fig. 1). The study also demonstrated that vitamin D treatment facilitated an increase in M2 macrophage with no observed hypercalcemia (Fig. 2). Based on this, we then detected if vitamin D could protect the CS-induced lung injury. The results showed that vitamin D alleviated CS-induced lung inflammatory injury. Reduced inflammation was characterized by secreting anti-inflammatory cytokines, inhibiting cell apoptosis and accelerating recovery from a progressive lung injury (Fig. 3). Finally, our *in vitro* studies delineated a mechanism by which vitamin D mediates resolution of CS-induced injury through activation of autophagy mainly in M2 macrophage (Figs. 4, 5) using Atg7<sup>-/-</sup> mice.

As one of the most important target organs, lung tissue defenses many hazard factors such as crystalline silica through macrophage, who acts as the key player regulating toxicant-caused tissue inflammation. Macrophages are heterogeneous and commonly exist in two distinct subsets (M1&M2) by the surrounding micro-environment stimuli (Shapouri-Moghaddam et al., 2018). M1 macrophage usually shows a pro-inflammatory effect while M2 macrophage produces anti-inflammatory cytokines (Smith et al., 2017). In this study, we reported that vitamin D treatment facilitated an increase in M2:M1 macrophage ratio to tip the balance towards attenuated inflammation (Figs. 1–3). Moreover, we revealed that vitamin D supported expansion of anti-inflammatory M2 macrophages due to enhance autophagy in M2 macrophages (Figs. 2–4).

As we all know, autophagy is the major intracellular degradation system, which plays an important role in regulating numerous inflammatory diseases (Bhattacharya et al., 2015; Racanelli et al., 2018). Enhanced autophagy especially in macrophages has been shown to protect from acute and chronic organ injury through attenuation of inflammation, promoting cell survival (Qiu et al., 2019). Consistently, in this study, vitamin D was found to trigger M2 autophagy, which mitigated CS-induced excessive pro-inflammation cytokines release and macrophages apoptosis, resulting in reduced production of inflammatory factors, consequently decreasing inflammatory infiltration and tissue damage.

However, disruption of autophagy or deficiency in autophagy genes contributes to a wide variety of disease pathologies including chronic inflammation, tumor progression and cancer (Liu et al., 2015; Li et al., 2020; Yang, 2020). Atg7 gene encodes an E1-like enzyme that is specifically involved in autophagosome formation and is essential for autophagy (Zhang et al., 2009). The reduction in Atg7 protein level has

been implicated as a causative factor in the autoimmune and neurodegenerative diseases by leading to reduced autophagic function (Komatsu et al., 2006). Using the myeloid-specific Atg7 deficient mice (design as Atg7<sup>-/-</sup>), we investigated the functional importance of macrophage autophagy in CS-induced lung injury. Data obtained from our Atg7<sup>-/-</sup> mice studies showed the enlarged damage after CS exposure. Moreover, macrophages polarization to M2 induced by vitamin D was slashed, which eroded the protective effects of vitamin D. In addition, we also found that deficiency of Atg7 impaired the capacity of anti-oxidant, manifesting as down-regulated Nrf2 signaling pathway and decreased level of GSH/GSSG, which defenses oxidative and inflammatory injury.

Although covering data from studies found that vitamin D has immunomodulatory effects in various diseases, this is the original study to identify its regulation on macrophage autophagy to intervene CS-caused lung inflammation. Findings from our study uncover the mechanism of vitamin D relieved inflammatory injury and adequately affirmed its application to anti-inflammation. Specifically, vitamin D inversed CS-induced macrophages infiltration and restored anti-inflammatory M2 macrophages in an autophagy dependent manner. Taken together, vitamin D-enhanced autophagy in macrophages can be potentially utilized for CS-caused pulmonary inflammatory injury.

#### CRediT authorship contribution statement

**Youjing Yang:** Methodology, Validation, Writing – original draft, Writing – review & editing. **Shuhui Wei:** Methodology, Software, Formal analysis, Data curation. **Kaimiao Chu:** Methodology, Software, Formal analysis, Data curation. **Qianmin Li:** Software, Methodology. **Yujia Zhou:** Software, Investigation. **Yu Ma:** Software, Methodology. **Lian Xue:** Resources. **Hailin Tian:** Resources. **Shasha Tao:** Conceptualization, Visualization, Writing – review & editing, Supervision, Project administration.

#### Declaration of Competing Interest

The authors declare that there is no known competing financial interests or personal relationships that could have appeared to influence the work reported in this paper.

#### Acknowledgement

The grants that supported our study are as follows: National Natural Science Foundation of China (Grant ref: 81703205); A project funded by the Priority Academic Program Development of Jiangsu Higher Education Institutions (PAPD); Foundation from Chongqing Yuzhong District Science and Technology Bureau (201930) and the Natural Science Foundation of Chongqing (cstc2020jcyj-msxm3187).

#### Appendix A. Supporting information

Supplementary data associated with this article can be found in the online version at [doi:10.1016/j.ecoenv.2021.112730](https://doi.org/10.1016/j.ecoenv.2021.112730).

#### References

- Barmania, S., 2016. Deadly denim: sandblasting-induced silicosis in the jeans industry. *Lancet Respir. Med.* 4 (7), 543.
- Berridge, M.J., 2017. Vitamin D deficiency accelerates ageing and age-related diseases: a novel hypothesis. *J. Physiol.* 595 (22), 6825–6836.
- Bhattacharya, A., et al., 2015. Autophagy is required for neutrophil-mediated inflammation. *Cell Rep.* 12 (11), 1731–1739.
- Cao, Y., et al., 2015. Loss of autophagy leads to failure in megakaryopoiesis, megakaryocyte differentiation, and thrombopoiesis in mice. *Exp. Hematol.* 43 (6), 488–494.
- Clarke, A.J., Simon, A.K., 2019. Autophagy in the renewal, differentiation and homeostasis of immune cells, 19(3): pp. 170–183.
- Das, L.M., et al., 2019. Vitamin D improves sunburns by increasing autophagy in M2 macrophages, 15(5): pp. 813–826.

- Deretic, V., Saitoh, T., Akira, S., 2013. Autophagy in infection, inflammation and immunity. *Nat. Rev. Immunol.* 13 (10), 722–737.
- Dong, J., Ma, Q., 2016. Myofibroblasts and lung fibrosis induced by carbon nanotube exposure, 13(1): p. 60.
- Du, S., et al., 2019. Dioscin alleviates crystalline silica-induced pulmonary inflammation and fibrosis through promoting alveolar macrophage autophagy. *Theranostics* 9 (7), 1878–1892.
- Fazzi, F., et al., 2014. TNFR1/phox interaction and TNFR1 mitochondrial translocation Thwart silica-induced pulmonary fibrosis. *J. Immunol.* 192 (8), 3837–3846.
- Glick, D., Barth, S., Macleod, K.F., 2010. Autophagy: cellular and molecular mechanisms. *J. Pathol.* 221 (1), 3–12.
- Guo, Y., et al., 2021. Effects of oral vitamin D supplementation on inflammatory bowel disease: a systematic review and meta-analysis.
- Hamilton Jr., R.F., Thakur, S.A., Holian, A., 2008. Silica binding and toxicity in alveolar macrophages. *Free Radic. Biol. Med.* 44 (7), 1246–1258.
- Holmes, D., 2017. NAFLD: vitamin D-induced autophagy prevents steatosis. *Nat. Rev. Endocrinol.* 13 (4), 190.
- Hu, Q., et al., 2021. Extracellular vesicle activities regulating macrophage- and tissue-mediated injury and repair responses. *Acta Pharm. Sin. B* 11 (6), 1493–1512.
- Høyer-Hansen, M., Nordbrandt, S.P., Jäättelä, M., 2010. Autophagy as a basis for the health-promoting effects of vitamin D. *Trends Mol. Med.* 16 (7), 295–302.
- Ilyas, G., et al., 2016. Macrophage autophagy limits acute toxic liver injury in mice through down regulation of interleukin-1 $\beta$ . *J. Hepatol.* 64 (1), 118–127.
- Komatsu, M., et al., 2005. Impairment of starvation-induced and constitutive autophagy in Atg7-deficient mice. *J. Cell Biol.* 169 (3), 425–434.
- Komatsu, M., et al., 2006. Loss of autophagy in the central nervous system causes neurodegeneration in mice. *Nature* 441 (7095), 880–884.
- Lai, H., et al., 2018. Combined effect of silica dust exposure and cigarette smoking on total and cause-specific mortality in iron miners: a cohort study. *Environ. Health* 17 (1), 46.
- Leung, C.C., Yu, I.T., Chen, W., 2012. Silicosis. *Lancet* 379 (9830), 2008–2018.
- Levine, B., Mizushima, N., Virgin, H.W., 2011. Autophagy in immunity and inflammation. *Nature* 469 (7330), 323–335.
- Li, C., et al., 2017. Dioscin exerts protective effects against crystalline silica-induced pulmonary fibrosis in mice. *Theranostics* 7 (17), 4255–4275.
- Li, M., et al., 2021. Macrophage related chronic inflammation in non-healing wounds. *Front. Immunol.* 12, 681710.
- Liu, K., et al., 2015. Impaired macrophage autophagy increases the immune response in obese mice by promoting proinflammatory macrophage polarization. *Autophagy* 11 (2), 271–284.
- Li, Z.L., et al., 2020. Autophagy deficiency promotes triple-negative breast cancer resistance to T cell-mediated cytotoxicity by blocking tenascin-C degradation, 11(1): p. 3806.
- Mantovani, A., Sica, A., Locati, M., 2005. Macrophage polarization comes of age. *Immunity* 23 (4), 344–346.
- Moreno-Vinasco, L., et al., 2014. Nicotinamide phosphoribosyltransferase inhibitor is a novel therapeutic candidate in murine models of inflammatory lung injury. *Am. J. Respir. Cell Mol. Biol.* 51 (2), 223–228.
- Parzych, K.R., Klionsky, D.J., 2014. An overview of autophagy: morphology, mechanism, and regulation. *Antioxid. Redox Signal.* 20 (3), 460–473.
- Qiu, P., Liu, Y., Zhang, J., 2019. Review: the role and mechanisms of macrophage autophagy in sepsis. *Inflammation* 42 (1), 6–19.
- Qi, Y.Y., Zhou, X.J., Zhang, H., 2019. Autophagy and immunological aberrations in systemic lupus erythematosus. *Eur. J. Immunol.* 49 (4), 523–533.
- Racanelli, A.C., et al., 2018. Autophagy and inflammation in chronic respiratory disease. *Autophagy* 14 (2), 221–232.
- Ritchie, M.E., et al., 2015. limma powers differential expression analyses for RNA-sequencing and microarray studies. *Nucleic Acids Res.* 43 (7), e47.
- Saitoh, T., Akira, S., 2016. Regulation of inflammasomes by autophagy. *J. Allergy Clin. Immunol.* 138 (1), 28–36.
- Sayan, M., Mossman, B.T., 2016. The NLRP3 inflammasome in pathogenic particle and fibre-associated lung inflammation and diseases. *Part Fibre Toxicol.* 13 (1), 51.
- Shang, L., et al., 2021. SS-31 protects liver from ischemia-reperfusion injury via modulating macrophage polarization, 2021: p. 6662156.
- Shapouri-Moghaddam, A., et al., 2018. Macrophage plasticity, polarization, and function in health and disease, 233(9): pp. 6425–6440.
- Shibutani, S.T., et al., 2015. Autophagy and autophagy-related proteins in the immune system. *Nat. Immunol.* 16 (10), 1014–1024.
- Smith, T.D., et al., 2017. Harnessing macrophage plasticity for tissue regeneration. *Adv. Drug Deliv. Rev.* 114, 193–205.
- Steenland, K., Ward, E., 2014. Silica: a lung carcinogen. *CA Cancer J. Clin.* 64 (1), 63–69.
- Tao, S., et al., 2019. Vitamin D protects against particles-caused lung injury through induction of autophagy in an Nrf2-dependent manner. *Environ. Toxicol.* 34 (5), 594–609.
- Tao, S., et al., 2013. Tanshinone I activates the Nrf2-dependent antioxidant response and protects against As(III)-induced lung inflammation in vitro and in vivo. *Antioxid. Redox Signal.* 19 (14), 1647–1661.
- The Lancet Respiratory, M., 2019. The world is failing on silicosis. *Lancet Respir. Med.* 7 (4), 283.
- Yang, Y., 2020. Autophagy promotes mammalian survival by suppressing oxidative stress and p53. *Nat. Commun.* 34 (9–10), 688–700.
- Yu, G., et al., 2012. clusterProfiler: an R package for comparing biological themes among gene clusters. *Omic* 16 (5), 284–287.
- Zhang, N., et al., 2021. A novel role of nogo proteins: regulating macrophages in inflammatory disease.
- Zhang, L., et al., 2014. N-acetylcysteine alleviated silica-induced lung fibrosis in rats by down-regulation of ROS and mitochondrial apoptosis signaling. *Toxicol. Mech. Methods* 24 (3), 212–219.
- Zhang, H., et al., 2019. Vitamin D protects against alcohol-induced liver cell injury within an NRF2-ALDH2 feedback loop. *Mol. Nutr. Food Res.* 63 (6), e1801014.
- Zhang, C., et al., 2019. Genome-wide mutation profiling and related risk signature for prognosis of papillary renal cell carcinoma. *Ann. Transl. Med.* 7 (18), 427.
- Zhang, Y., et al., 2009. Adipose-specific deletion of autophagy-related gene 7 (atg7) in mice reveals a role in adipogenesis. *Proc. Natl. Acad. Sci. USA* 106 (47), 19860–19865.